Inorganic Chemistry

Communication

pubs.acs.org/IC

Perovskite-Structured $PbTiO_3$ Thin Films Grown from a Single-Source Precursor

Muhammad Adil Mansoor,[†] Azhani Ismail,[†] Rosiyah Yahya,[†] Zainudin Arifin,[†] Edward R. T. Tiekink,[†] Ng Seik Weng,[†,‡] Muhammad Mazhar,*[,†] and Ali Reza Esmaeili[†]

[†]Department of Chemistry, Faculty of Science, University of Malaya, Lembah Pantai, 50603 Kuala Lumpur, Malaysia

[‡]Chemistry Department, Faculty of Science, King Abdulaziz University, P.O. Box 80203, 22254 Jeddah, Saudi Arabia

Supporting Information

ABSTRACT: Perovskite-structured lead titanate thin films have been grown on FTO-coated glass substrates from a single-source heterometallic molecular complex, $[PbTi(\mu_2\text{-}O_2CCF_3)_4(THF)_3(\mu_3\text{-}O)]_2$ (**1**), which was isolated in quantitative yield from the reaction of tetraacetatolead(IV), tetrabutoxytitanium(IV), and trifluoroacetic acid from a tetrahydrofuran solution. Complex **1** has been characterized by physicochemical methods such as melting point, microanalysis, FTIR, ^1H and ^{19}F NMR, thermal analysis, and single-crystal X-ray diffraction (XRD) analysis. Thin films of lead titanate having spherical particles of various sizes have been grown from **1** by aerosol-assisted chemical vapor deposition at 550 °C. The thin films have been characterized by powder XRD, scanning electron microscopy, and energy-dispersive X-ray analysis. An optical band gap of 3.69 eV has been estimated by UV−visible spectrophotometry.

Among ferroelectric, pyroelectric, and piezoelectric inorganic materials,[1] lead titanate is the most widely used in capacitors for energy storage, current blocking, electrical noise-filtering and high-frequency tuning devices, self-regulating electric heating systems, dynamic random access memories, nonvolatile memories and positive-temperature-coefficient resistors, sensors, actuators, and sound and ultrasound transducer and electrooptical devices.[2] The efficiency of these devices critically depends on the imperfection of the crystalline structure and the bulk and surface properties of the thin films.[3] Previously, lead titanate thin films have been prepared using various techniques, such as pulsed laser deposition,[4] chemical vapor deposition,[5] the sol−gel method,[6] coprecipitation,[7] and hydrothermal synthesis,[8] besides traditional solid-state reactions of mixed oxides. These deposition techniques suffer from multiple drawbacks, such as poor conformality, low throughput, restricted directional variation, and low compositional control. Several of these problems can be overcome by using aerosol-assisted chemical vapor deposition (AACVD) techniques. This method requires the precursor to be soluble in any solvent that is suitable for aerosol generation.[9] The precursor is dissolved in a solvent, and an aerosol of the solution is generated ultrasonically to deposit layers of the decomposed material on the target substrate while at the same time ensuring both reproducibility and the presence of all components of interest in the deposited layer(s).[10] Various researchers have used lead acetate and titanium alkoxide to make thin films by sol−gel techniques,[11] and in some cases, the isolation of molecular species (obtained from mixing metal alkoxides) for generating lead titanate thin films has been achieved.[12,13] Our attention has focused on the replacement of alkoxy groups with the more volatile trifluoroacetato (TFA) group to form complexes that are capable of delivering all constituents of interest[14] without carbonaceous contamination. Hence, we synthesized the heterobimetallic complex $[PbTi(\mu_2\text{-}O_2CCF_3)_4(C_4H_8O)_3(\mu_3\text{-}O)]_2$ (**1**), used it as a precursor for the growth of impurity-free thin films of $PbTiO_3$ on FTO-coated glass substrates by AACVD, and characterized the films for possible technical applications.

The structure of **1** was elucidated by X-ray crystallography,[15] with the first key result being the observation that lead had been reduced to lead(II) during the course of the reaction; see also the Supporting Information (SI). Views of the molecular structure are presented in Figure 1; displacement ellipsoid diagrams and

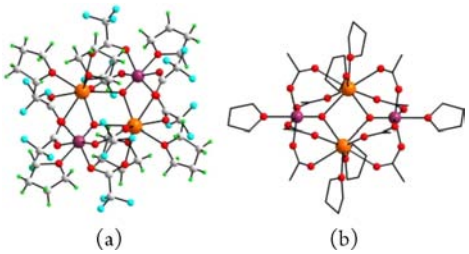

Figure 1. Two views of the molecular structure of **1**: (a) full molecule drawn with arbitrary ellipsoids; (b) molecule without F and H atoms (the organic residues are shown in stick form). The disordered components have been omitted for clarity. Color code: Pb, orange; Ti, violet; F, cyan; O, red; C, gray; H, green.

details of the disorder present in the structure are included in the SI. The asymmetric unit of complex **1** comprises two half molecules, with the complete molecule generated by the application of a center of inversion in each case. The core of the molecule is a Pb_2O_2 rhombus with almost equivalent Pb−O bond distances [range of Pb−O bond lengths for the two independent molecules: 2.652(4)−2.667(4) Å]. The O atoms of the core also coordinate to a Ti atom [Ti−O = 1.674(4)−1.669(4) Å], thereby functioning as μ_3-O ligands. Each Pb···Ti

Received: December 24, 2012
Published: April 29, 2013

   dx.doi.org/10.1021/ic302772b | *Inorg. Chem.* 2013, 52, 5624−5626

edge of the expanded $Pb_2O_2Ti_2$ core is bridged by two carboxylate ligands [Pb−O = 2.560(6)−2.726(6) Å; Ti−O = 1.999(4)−2.016(5) Å]. Finally, each Pb [Pb−O = 2.509(4)−2.722(5) Å] and Ti [Ti−O = 2.230(4)−2.232(4) Å] atom is coordinated by two and one THF molecules, respectively. It is apposite to compare the derived interatomic parameters with those of arguably the closest related heterometallic structure, namely, $[PbTi(\mu_3\text{-O-}i\text{-Pr})_2(\mu_2\text{-O-}i\text{-Pr})_4(\mu_4\text{-O})]_2$.[12] The Pb−O(O-*i*-Pr) bond lengths for pentacoordinate Pb in the latter range from 2.36(1) to 2.49(1) Å, i.e., considerably shorter than that in **1**, a result correlated with the higher coordination number in **1**; the range of Ti−O(O-*i*-Pr) bond lengths, 1.80(1)−2.20(1) Å, encompasses the range in **1**.

A description of the resultant eight-coordinate geometry for the Pb atoms is based on a square antiprism. One face is occupied by two μ_3-O and two carboxylate O atoms, whereas the other is defined by two carboxylate O and two THF O atoms; the lengths of the edges range from 2.94 to 3.30 Å. The dihedral angles between the faces are 5.47(14) and 3.62(15)° for the Pb1 and Pb2 polyhedra, respectively, indicating a parallel arrangement, and the rotation of the top to bottom faces is ca. 89° for the Pb1 atom and ca. 88° for the Pb2 atom. The coordination polyhedron for each of the Ti1 and Ti2 atoms is based on an octahedron. The major distortions are manifested in the deviations of the trans angles subtended by carboxylate O atoms [160.0(2) and 157.52(19)°, respectively].

The framework in **1**, whereby a $M_2O_2M'_2$ core with each of the four M···M′ edges bridged by two carboxylate ligands and with additional O donors (two for M and one for M′), appears to be unprecedented in the crystallographic literature, as revealed by a search of the Cambridge Crystallographic Database.[16] The most closely related structure is that of $[U_4(O_2CF_3)_{16}(OH_2)_2]$, isolated as a 1:2 cocrystal with 4,7,13,16,21,24-hexaoxa-1,10-diazabicyclo[8.8.8]hexacosane.[17] Here, M = M′ = U, with each edge bridged by two carboxylate ligands. However, allowing for charge, this is where the similarity between the two structures ends. The μ_3-O atoms of the core in **1** are replaced by μ_3-OH_2 ligands. The four THF O atoms connected to the Pb atoms in **1** are now in the form of two additional bridging carboxylate ligands. Finally, each Ti−O(THF) bond in **1** is replaced by three monodentate carboxylate ligands.

The thermal behavior of **1** has been examined by thermogravimetric analysis (TGA) performed under an inert atmosphere of flowing nitrogen gas (25 cm^3/min) with a heating rate of 10 °C/min. The TGA/differential thermogravimetry (DTG) of precursor **1** shows systematically five distinct stages of weight losses at 105−119, 125, 191, 319, and 530 °C (Figure 2). The thermal degradation of **1** begins slowly with successive losses of two THF molecules in the temperature range of 60−119 °C, showing a weight losses of 3.7 and 7.6%, respectively. The third THF molecule is lost at 125 °C corresponding to a weight loss of 10.8%. The remaining three out of a total of six THF molecules are lost at the higher temperature of 191 °C. Immediately after the loss of all six THF molecules, the core of **1** starts to collapse at 191 °C and degradation is completed at 350 °C, yielding a residue of 34.3% that corresponds to the formation of a Pb_2O_3/TiO_2 composite. This composite partially decomposes to $PbTiO_3$, PbO, and TiO_2 at 400 °C.[18] This observation is supported by powder X-ray diffraction (XRD) of the sample obtained from calcination of the precursor at 300, 350, and 400 °C (Figure S3a in the SI). A further rise in temperature to 530 °C yields a stable residue with a 0.9% weight loss. This small loss in weight corresponds to a loss of oxygen from the Pb_2O_3/TiO_2 composite to finally yield stable ash of $PbTiO_3$. Further heating of the residue to 850 °C did not bring any change in weight, indicating complete decomposition of **1** to furnish a 33.4% residual weight, as expected for $PbTiO_3$. The CHN analysis and Fourier transform (FTIR) spectra of the TGA residue indicate the removal of carbonaceous matter from the organic groups, leaving a final residue corresponding to metal oxides. The FTIR absorption bands at 507 and 748 cm^{-1} are in close agreement with the reported data for the Ti−O and Pb−O stretching modes of vibration, respectively.[19] In the core of precursor **1**, each Pb and Ti center is coordinatively saturated by the O atoms of chelating TFA ligands and μ_3-O, which eliminates the need for additional oxygen from an extraneous source to form oxides. Thus, the new precursor is a suitable single-source precursor for the deposition of thin films of $PbTiO_3$ at a relatively low temperature of 550 °C (Scheme S1 in the SI).

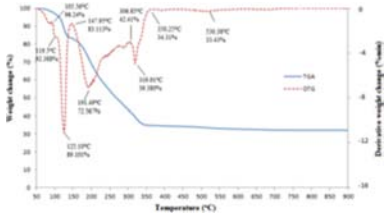

Figure 2. TGA/DTG curves showing thermal decomposition of precursor **1** to a stable $PbTiO_3$ residue.

$PbTiO_3$ films generated from precursor **1** (section S1 in the SI) were further studied by powder XRD spectroscopy. $PbTiO_3$ has a tetragonal crystal system with space group *P4/mmm* and lattice dimensions of $a = b = 3.8993$ Å and $c = 4.1532$ Å. The diffractogram of the decomposition product (Figure S3c in the SI) with peaks corresponding to $PbTiO_3$ (ICDD 00-006-0452) shows a close correspondence. In the XRD pattern, the peaks at $2\theta = 21.39$, 22.78, 31.45, 32.43, 39.05, 43.56, 46.53, 49.69, 51.75, 52.42, 55.36, 57.26, 65.63, 67.93, 70.47, 72.15, 72.38, 72.67, 76.78, and 77.30° correspond to $PbTiO_3$. The XRD pattern of the thin films deposited at 550 °C showed no evidence for the formation of any lead and titanium oxides or any other form of lead titanates, indicating that the precursor **1** is a potential candidate for the deposition of crystalline $PbTiO_3$. The light-brown transparent, uniform, robust, and stable toward atmospheric conditions thin films of $PbTiO_3$ can be grown by AACVD on an FTO-conducting glass substrate under argon gas flow at a rate of 150 cm^3/min at 550 °C. The grown thin films appear strongly adhered to an FTO glass substrate because they pass the scotch-tape test.[20]

The surface morphology and thickness of $PbTiO_3$ thin films grown on FTO glass substrates were investigated by field-emission scanning electron microscopy (FESEM) and profilometry (KLA Tencore $P\bar{6}$ surface profiler), as presented in Figure 3. The films deposited at 550 °C have a thickness of 340 nm and are generally smooth, fine-grained, varying in grain size from 0.3 to 1 μm with a glassy appearance. The glowing appearance in these fine grains suggests light remittance after absorption. The average number of larger particles is more than that of smaller particles in the thin films. Such fine-grained structures are generally desirable from the standpoint of photoelectrical and photocatalytic applications. Energy-dispersive X-ray analysis (Figure S4 in the SI) of the powder obtained from calcination of the precursor at 550 °C and of spherical

dx.doi.org/10.1021/ic302772b | *Inorg. Chem.* 2013, 52, 5624−5626

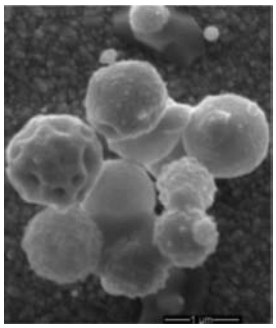

Figure 3. SEM image of a thin film of $PbTiO_3$ deposited from **1** showing transparent spherical particles with a glassy appearance.

particles of thin films confirmed the parent composition of the material to be $PbTiO_3$.

The optical absorption spectrum of thin films was recorded on a Lambda 35 Perkin-Elmer UV−visible spectrophotometer in the wavelength range of 300−900 nm using a similar FTO-coated glass substrate as a reference to exclude the substrate contribution in the spectrum. The UV−visible spectrum of the $PbTiO_3$ thin film shows a sharp absorption edge at 324 nm, and the band gap was calculated as a Tauc plot of $(\alpha h\nu)^2$ versus energy, giving a value of 3.69 eV for the direct band gap, which is in good agreement with the reported value of 3.60 eV (Figure 4).[21]

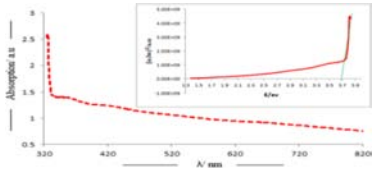

Figure 4. UV−visible absorption spectra between absorption and wavelength [inset: Tauc plot of $(\alpha h\nu)^2$ versus energy] of $PbTiO_3$ thin films deposited from precursor **1** using AACVD showing a sharp absorption edge at 324 nm.

Single-source heterometallic complex **1** can be synthesized by a simple and routine chemical reaction of tetraacetatolead(IV), tetrabutoxytitanium(IV), and trifluoroacetic acid in THF under standard reaction conditions and has been characterized by various analytical methods. Complex **1** is unique in the sense that it contains all of the necessary components of $PbTiO_3$ bonded in one structure and thermally decomposes at 550 °C under mild AACVD conditions to yield thin films of crystalline material $PbTiO_3$ having a band gap of 3.69 eV that may be used for various technological and photocatalytic applications.

■ ASSOCIATED CONTENT

Supporting Information

X-ray crystallographic data for complex **1** in CIF format, figures, decomposition scheme, analysis of the experiment, conditions and results, and our work details (section S1), and details of the modeling of the disorder and molecular structure diagrams (section S2). This material is available free of charge via the Internet at http://pubs.acs.org.

■ AUTHOR INFORMATION

Corresponding Author

*E-mail: mazhar42pk@yahoo.com. Phone: +60 03 79674269. Fax: +60 03 79674193. Mobile: +60 16 2796040.

Notes

The authors declare no competing financial interest.

■ ACKNOWLEDGMENTS

M.M. acknowledges the High-Impact Research Grant UM.C/625/1/HIR/131 and the UMRG Grant RG097/10AET for funding this research. The Ministry of Higher Education (Malaysia) is thanked for funding structural studies through the High-Impact Research scheme (Grant UM.C/HIR-MOHE/SC/3 to E.R.T.T.).

■ REFERENCES

(1) (a) Cai, Z.; Xing, X.; Yu, R.; Sun, X.; Liu, G. *Inorg. Chem.* **2007**, *46*, 7423. (b) Cho, S. B.; Noh, J. S.; Lencka, M. M.; Riman, R. E. *J. Eur. Ceram. Soc.* **2003**, *23*, 2323.
(2) Lee, C. Y.; Tai, N.-Y.; Sheu, H. S.; Chiu, H. T.; Hsieh, S. H. *Mater. Chem. Phys.* **2006**, *97*, 468.
(3) Setter, N.; Damjanovic, D.; Eng, L.; Fox, G.; Gevorgian, S.; Hong, S.; Kingon, A.; Kohlstedt, H.; Park, N. Y.; Stephenson, G. B.; Stolitchnov, I.; Tagantsev, A. K.; Taylor, D. V.; Yamada, T.; Streiffer, S. *J. Appl. Phys.* **2006**, *100*, 051606.
(4) Chaouia, N.; Millona, E.; Mullera, J. F.; Eckerb, P.; Bieckb, W.; Migeonb, H. N. *Mater. Chem. Phys.* **1999**, *59*, 114.
(5) Pan, C.; Tsai, D.; Hong, L. *Mater. Chem. Phys.* **2001**, *70*, 223.
(6) Hernandez-Sanchez, B. A.; Chang, K. S.; Scancella, M. T. *Chem. Mater.* **2005**, *17*, 5905.
(7) Safari, A.; Lee, Y. H.; Halliyal, A.; Newnham, R. E. *Am. Ceram. Soc. Bull.* **1987**, *66*, 668.
(8) Cheng, H.; Ma, J.; Zhao, Z. *Chem. Mater.* **1994**, *6*, 1033.
(9) Brethon, A.; Hubert-Pfalzgraf, L. G.; Daran, J. C. *Dalton Trans.* **2006**, 250.
(10) Veith, M.; Haas, M.; Huch, V. *Chem. Mater.* **2005**, *17*, 95.
(11) Hendricks, W. C.; Desu, S. B.; Peng, C. H. *Chem. Mater.* **1994**, *6*, 1955.
(12) Daniele, S. C.; Papiernik, R.; Hubert-Pfalzgraf, L. G. *Inorg. Chem.* **1995**, *34*, 628.
(13) Veith, M.; Bender, M.; Lehnert, T.; Zimmer, M.; Jakob, A. *Dalton Trans.* **2011**, *40*, 1175.
(14) Tahir, A. A.; Hamid, M.; Mazhar, M.; Zeller, M.; Hunter, A. D. *New J. Chem.* **2009**, *33*, 1535.
(15) Crystal data for complex **1**: $C_{40}H_{48}F_{24}O_{24}Pb_2Ti_2$ (1878.96), triclinic, $P\bar{1}$, a = 12.8283(4) Å, b = 12.8833(3) Å, c = 21.4442(4) Å, α = 101.583(2)°, β = 93.234(2)°, γ = 118.803(3)°, V = 2993.57(13) Å^3, Z = 2, T = 100(2) K, λ(Mo Kα) = 0.71073 Å, 48414 reflections collected, 13815 unique (R_{int} = 0.038), 11477 with $I > 2\sigma(I)$, R1 = 0.043 (obsd data), wR2 = 0.114 (all data). CCDC deposition number: 884630.
(16) Allen, F. H. *Acta Crystallogr.* **2002**, *B58*, 380.
(17) Charpin, P.; Folcher, G.; Nierlich, M.; Lance, M.; Vigner, D.; Navaza, A.; de Rango, C. *Acta Crystallogr.* **1990**, *C46*, 1778.
(18) Wittry, D. B. U.S. Patent 4,009,919, 1978.
(19) Tang, X. G.; Guo, H. K.; Zhou, Q. F.; Zhang, J. X. *Nanostruct. Mater.* **1998**, *2*, 161.
(20) Larsen, P. K.; Cuppens, R.; Sprerings, G. A. C. M. *Ferroelectrics* **1992**, 128.
(21) Zametin, V. I. *Phys. Status Solidi B* **1984**, *124*, 625.